2024 IEEE-APS Topical Conference on Antennas and Propagation in Wireless Communications (APWC) | 979-8-3503-6077-6/24/$31.00 ©2024 IEEE | DOI: 10.1109/APWC61918.2024.10701980

Wideband Joint Elevation-Azimuth Angle Estimation Based on Multiple Frequency Model and Atomic Norm Minimizaion

1st Jingming Zhang
Institute of Acoustics
Chinese Academy of Sciences
Beijing, China
University of Chinese Academy of Sciences
Beijing, China
zhangjingming@mail.ioa.ac.cn

2nd Min Wu
Institute of Acoustics
Chinese Academy of Sciences
Beijing, China
University of Chinese Academy of Sciences
Beijing, China
wumin880902@hotmail.com

3rd Chengpeng Hao*
Institute of Acoustics
Chinese Academy of Sciences
Beijing, China
University of Chinese Academy of Sciences
Beijing, China
haochengp@mail.ioa.ac.cn

4th Da Xu
Institute of Acoustics
Chinese Academy of Sciences
Beijing, China
University of Chinese Academy of Sciences
Beijing, China
xuda@mail.ioa.ac.cn

***Abstract*—The estimation of the Direction of Arrival (DOA) plays a critical role in sonar, radar, and acoustic source localization. However, current research predominantly concentrates on narrowband, one-dimensional signals, which can't be directly applied to practical scenarios where the signals are usually wideband and multi-dimensional. In this paper, we propose a two-dimensional multi-frequency atomic norm minimization (2DMFANM) algorithm for the estimation of elevation and azimuth angles for wideband signals. A multi-frequency signal representation is adopted to accurately model wideband signals. The technique of atomic norm minimization (ANM) is leveraged to extract DOA information from the received signals in a gridless fashion. To transform the intractable ANM formulation into a solvable semi-definite programming (SDP) problem, we conduct a thorough analysis of the corresponding dual problem. Subsequently, we introduce a novel two-dimensional mapping operator, which aids in the construction of a multivariate trigonometric polynomial representation. This formulation is specifically designed to facilitate the application of the bounded lemma, thereby enabling the transformation of the ANM problem into the SDP framework. Compared with narrowband ANM methods, 2DMFANM takes advantage of additional data from multiple frequencies and remarkably improves the accuracy of estimation. Numerical simulations are executed and demonstrate the superior performance of our proposed method than existing algorithms.**

***Index Terms*—wideband signals, multi-frequency, ANM, 2D DOA estimation, SDP**

I. Introduction

Direction of Arrival (DOA) estimation has been a crucial research area in array signal processing [1] with applications spanning sonar [2], radar [3], and sound source localization [4]. In order to exceed the resolution limit imposed by the array's aperture [5] – [8], subspace-based super-resolution techniques, such as Multiple Signal Classification (MUSIC) [9] [10] and Estimation of Signal Parameters via Rotational Invariance Techniques (ESPRIT) [11] were proposed. These methods exceeded the Rayleigh limit, significantly enhancing resolution. The subspace based methods depend on the assumption of source independence, which makes them sensitive to signal coherence and can result in incomplete estimations. They also require a large number of snapshots to ensure the reliability of the estimated covariance matrix, constraining their practical applications.

Recently, the theory of compressed sensing(CS) [12] [13] had been applied to the field of DOA estimation [14]. By densely gridding the DOA region, steering vectors corresponding to each grid point can form an overcomplete dictionary, transforming the DOA estimation problem into one of sparse recovery [15] [16]. The CS-based methods can recover the desired DOAs with limited data, even in the scenarios where only single snapshot is available. The aforementioned methods presume that the DOAs are on a predefined grid, hence termed on-grid algorithms. Off-grid scenarios, which are common in practice, can lead to grid mismatch issues. Chi et al. [17] analyzed the impact of grid mismatch, and Zhang et al. [18]

This work was supported by the National Natural Science Foundation of China(62371446,62001468,61971412,62201623) and Youth Innovation Promotion Association CAS(2023030).

pointed out that in joint localization scenarios with multiple arrays, grid mismatch could result in target omissions, significantly degrading localization performance. Consequently, various off-grid algorithms have been developed to mitigate grid mismatch effect [19] – [22]. However, these methods still imply the existence of a grid, thus complicating the accurate estimation of continuous DOAs.

Currently, gridless approaches conducting direct continuous DOA estimation have been proposed. Candes et al. [23] demonstrated that perfect frequency extension could be achieved from low-frequency time sampling through total variation minimization, equivalent to atomic norm minimization (ANM). Tang et al. [24] explored spectral estimation under random partial observations and established that with a sample size exceeding $O(r \log r \log n)$, the estimation through ANM is likely to be accurate.

Despite these advancements, existing methods primarily consider one-dimensional narrowband signals. In practical scenarios, the signals received are typically wideband and multidimensional [25] [26]. Therefore, it is crucial to adapt current narrowband, one-dimensional techniques to wideband, multi-dimensional contexts. Expanding ANM to higher dimensions, Chi et al. [27] utilized a two-level Toeplitz matrix for two-dimensional extension, and Yang et al. [28] leveraged a multi-level Toeplitz matrix structure for higher-dimensional ANM. The application of ANM to wideband signals was also explored by Wu et al. [29], who employed a multi-frequency model for DOA estimation. However, the use of gridless techniques for multi-dimensional wideband signals has received limited attention.

In this paper, we introduce a novel wideband joint elevation-azimuth angle estimation algorithm based on ANM. A multi-frequency model is adopted to represent wideband signals and a corresponding atomic set is proposed. To transform the original ANM problem into a tractable semidefinite programming (SDP) problem, we investigate the dual problem of ANM and propose a two-dimensional mapping operator. We also provide the SDP form of the primal problem derived from the dual SDP, from which the angular frequencies are retrieved using the MaPP [28] algorithm. The elevation and azimuth angles are then calculated from these frequencies.

The paper is organized as follows: section II introduces the two-dimensional multi-frequency model describing the signals received; section III presents the proposed 2DMFANM algorithm; section IV conducts numerical experiments to demonstrate the proposed algorithm's superior performance; and section V concludes with a discussion of the results and potential avenues for future research.

Notations

$(\cdot)^T, (\cdot)^H$ stand for symmetric and Hermitian transpose, respectively. $< \cdot, \cdot >_{\mathbb{R}}$ stands for real inner product. $\otimes$ and $\odot$ stand for Kronecker product and Khatri-Rao product, respectively.

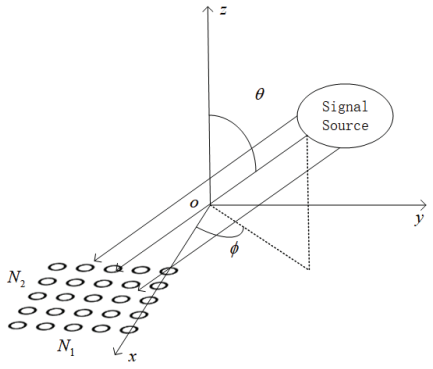

Fig. 1. Geometry of Array Configuration

II. Signal Model

Consider r wideband underwater acoustic waves, originating from the far-field, impinging upon an $N_1 \times N_2$ uniform rectangular array (URA) of hydrophones. The array consists of N_1 elements along the x-axis and N_2 elements along the y-axis. The elevation and azimuth angles of the k-th wave are denoted by θ_k and ϕ_k, respectively, as illustrated in Fig. 1. For any independent sound source, the wideband signal can be represented in the form of multiple frequencies using off-the-shelf spectral analysis techniques, such as the Discrete Fourier Transform (DFT) and filter bank methods. Assume a total of N_f subbands, with the central frequency of each subband defined as $f \cdot f_0$, where $f \in \{1, 2, ..., N_f\}$. The i-th source signal, $s_i = c_i \cdot [{p_i}^1, p_i^2, ..., {p_i}^{N_f}] = c_i p_{\omega_i}^T$, can then be expressed as

$$s_i = c_i \cdot [{p_i}^1, p_i^2, ..., {p_i}^{N_f}] = c_i p_{\omega_i}^T, \tag{1}$$

where $p_{\omega_i}^T \triangleq [{p_i}^1, p_i^2, ..., {p_i}^{N_f}]$, $\|p_{\omega_i}\| = 1$, and $p_{\omega_i}^T \triangleq [{p_i}^1, p_i^2, ..., {p_i}^{N_f}]$, $\|p_{\omega_i}\| = 1$. Here, c_i represents the signal amplitude, and p_{ω_i} comprises the power across N_f frequency bins. Let $J = \{0, 1, \ldots, N_1 - 1\} \times \{0, 1, \ldots, N_2 - 1\}$ be the set of array element indices, defined as $J = \{0, 1, \ldots, N_1 - 1\} \times \{0, 1, \ldots, N_2 - 1\}$. The signal received by the k-th element in the f-th subband can then be expressed as

$$x_k^f = x_{(k_1,k_2)}^f = \sum_{i=1}^{r} c_i \exp\left(j2\pi f f_0 \cdot \frac{d}{c}[\cos(\phi_i)\sin(\theta_i), \sin(\phi_i)\sin(\theta_i)]k\right) \cdot p_i^f, \tag{2}$$

where $k \in J$, c represents the underwater acoustic velocity, and d denotes the interspacing of the array elements.

Define the angular frequency vector as $\omega_i = [\omega_{1i}, \omega_{2i}] \triangleq f_0 \cdot \frac{d}{c}[\cos(\phi_i)\sin(\theta_i), \sin(\phi_i)\sin(\theta_i)]^T$, we have

$$x_k^f = x_{(k_1,k_2)}^f = \sum_{i=1}^{r} c_i \exp\left(j2\pi f \omega_i^T k\right) \cdot p_i^f. \tag{3}$$

Note that the angular information, comprising the elevation and azimuth angles, can be retrieved by accurately determining ω_i. Combining signals calculated from N_f subbands, the signal received by the k-th element can be put together as

$$\begin{aligned} x_k &= \left[x_k^1, x_k^2, \ldots, x_k^f\right] \\ &= \sum_{i=1}^{r} c_i \cdot [\exp(j2\pi {\omega_i}^T k), ..., \exp(j2\pi N_f {\omega_i}^T k)] \odot [p_i^1, ..., p_i^f] \\ &= \sum_{i=1}^{r} c_i \cdot [\exp(j2\pi {\omega_i}^T k), ..., \exp(j2\pi N_f {\omega_i}^T k)] \odot p_{\omega_i}^T. \end{aligned} \tag{4}$$

When the signals received by all array elements on the f-th subband are aggregated, the resulting matrix representation is as follows

$$X^f = \begin{bmatrix} x_{00}^f & x_{10}^f & ... & x_{(N_1-1)0}^f \\ x_{01}^f & x_{11}^f & ... & x_{(N_1-1)1}^f \\ ... & ... & ... & ... \\ x_{0(N_2-1)}^f & x_{1(N_2-1)}^f & ... & x_{(N_1-1)(N_2-1)}^f \end{bmatrix}.$$

This can be further expressed as

$$\begin{aligned} X^f &= \sum_{i=1}^{r} (c_i {p_i}^f) \cdot a_2(f, \omega_{2i}) a_1(f, \omega_{1i})^T \\ &= \sum_{i=1}^{r} (c_i p_i^f) A(f, \omega_i). \end{aligned} \tag{5}$$

where $a_k(f, \omega_{ki}) = [1, \exp(j2\pi f \omega_{ki}), ..., \exp(j2\pi f \omega_{ki} \cdot (N_k - 1))$, for $k = 1, 2$, represent the steering vectors. The matrix $A(f, \omega_i)$ is defined as: $A(f, \omega_i) = a_2(f, \omega_{2i}) \cdot a_1(f, \omega_{1i})^T$. Vectorizing equation (5) leads to the following representation for the f-th subband:

$$\tilde{x}^f \triangleq vec(X^f) = \sum_{i=1}^{r} (c_i p_i^f) a_1(f, \omega_{1i}) \otimes a_2(f, \omega_{2i}). \tag{6}$$

By integrating equations (4) and (6), we obtain the complete signal model

$$\begin{aligned} \tilde{X} &\triangleq [\tilde{x}^1, \tilde{x}^2, ...\tilde{x}^{N_f}] \\ &= \sum_{i=1}^{r} c_i [\tilde{a}(1, \omega_i), \tilde{a}(2, \omega_i), ..., \tilde{a}(N_f, \omega_i)] \odot {p_{\omega_i}}^T \\ &= \sum_{i=1}^{r} c_i \tilde{A}(\omega_i) \odot {p_{\omega_i}}^T, \end{aligned} \tag{7}$$

where $\tilde{A}(\omega_i) \triangleq [\tilde{a}(1, \omega_i), \tilde{a}(2, \omega_i), ..., \tilde{a}(N_f, \omega_i)]$.

In this paper, $\tilde{X}$ represents the signal from which the desired DOA information is to be extracted. In scenarios absent of noise, we handle $\tilde{X}$ directly. However, in practical situations where the presence of noise cannot be disregarded, the received signal is modeled as

$$\tilde{Y} = \tilde{X} + N, \tag{8}$$

where N denotes the noise component. This model acknowledges the reality of signal processing environments and lays the groundwork for subsequent noise mitigation techniques to be applied in the process of DOA estimation.

III. 2DMFANM Algorithm

In this section, we present our 2DMFANM algorithm and use it for joint elevation-azimuth angle estimation.

Inspired by the form of equation (7) and drawing upon the work of Wu et al. [29], we define the atomic set $\mathbb{A}$ as follows

$$\mathbb{A} \triangleq \{\tilde{A}(\omega) \odot p_\omega^T | \omega \in [0, 1]^2, \|p_\omega\|_2 = 1\}. \tag{9}$$

This set, $\mathbb{A}$, encompasses all possible steering vectors modulated by a power pattern, with the constraint that the power pattern vector, p_ω, is normalized to have a unit Euclidean norm.

To extract DOA information from the observed signal, which is $\tilde{X}$ in the absence of noise or Y when noise is present, the proposed atomic norm minimization (ANM) problems are formulated as follows

For the noise-free case:

$$\min_{\tilde{X}} \|\tilde{X}\|_{\mathbb{A}}, \quad \text{s.t.} \quad Y = \tilde{X} \ . \tag{10}$$

For the noise-present case:

$$\min_{\tilde{X}} \|\tilde{X}\|_{\mathbb{A}}, \quad s.t. \quad \|Y - \tilde{X}\|_2 \leq \beta. \tag{11}$$

Here, the atomic norm $\|\tilde{X}\|_{\mathbb{A}}$ is defined as

$$\begin{aligned} \|\tilde{X}\|_{\mathbb{A}} &= \inf\{t \geq 0 | \tilde{X} \in t \cdot conv(\mathbb{A})\} \\ &= \inf\{\sum\nolimits_{\omega} |c_\omega| | \tilde{X} = \sum\nolimits_{\omega} c_\omega \tilde{A}(\omega) \odot {p_\omega}^T\}, \end{aligned} \tag{12}$$

where β represents the noise power. The atomic norm serves as a proxy for the l_0-norm in promoting sparsity, under the assumption that $\tilde{X}$ can be represented as a sparse combination of atoms from the set $\mathbb{A}$. The objective in the noise-free case is to find the sparsest representation of Y using the atoms in $\mathbb{A}$, whereas in the noise-present case, the objective is to find a representation that is both sparse and within a certain error tolerance β of the noisy observation Y.

Given that the atomic norm cannot be computed directly, the optimization problem must be reformulated as an SDP problem to enable a solution. The subsequent portion of this section will detail the conversion process of (10), pertaining to the noise-free case, into an SDP. Similarly, (11), addressing the case with noise, can be transformed into an SDP with minimal modifications.

The dual problem of (10) is

$$\max_Q < \tilde{X}, Q >_{\mathbb{R}}, \quad s.t. \quad \|Q\|_{\mathbb{A}}^* \leq 1, \tag{13}$$

where $\|\cdot\|_{\mathbb{A}}^*$ is the dual norm of the atomic norm defined in (12), which is defined as

$$\|Q\|_{\mathbb{A}}^* = \sup_{\|\tilde{X}\|_{\mathbb{A}} \leq 1} < Q, \tilde{X} >_{\mathbb{R}}. \tag{14}$$

Utilizing the definition of $\tilde{X}$ in (7) and defining $Q = [q_1, q_2, ..., q_{N_f}]$, it yields

$$\begin{aligned} \|Q\|_{\mathbb{A}}^* &= \sup_{\|\tilde{X}\|_{\mathbb{A}} \leq 1} < Q, \tilde{X} >_{\mathbb{R}} \\ &= \sup_{\omega, p_\omega} < Q, \tilde{A}(\omega) \odot p_\omega^T >_{\mathbb{R}} \\ &= \sup_{\omega, p_\omega} \operatorname{Re}(\sum_{f=1}^{N_f} p_\omega(f) q_f^H \tilde{a}(f, \omega)). \end{aligned} \tag{15}$$

Let $\Psi(Q,\omega) \triangleq [{q_1}^H \tilde{a}(1,\omega), {q_2}^H \tilde{a}(2,\omega), ..., {q_{N_f}}^H \tilde{a}(N_f,\omega)]^T$. We obtain

$$\begin{aligned} \|Q\|_{\mathbb{A}}^* &= \sup_{x_\omega,\omega} \mathrm{Re}(x_\omega^H \Psi(Q,\omega)) \\ &= \sup_{x_\omega,\omega} |x_\omega^H \Psi(Q,\omega)| \\ &= \sup_\omega \|\Psi(Q,\omega)\|_2. \end{aligned} \tag{16}$$

Inspired by the mapping operator proposed in [29], we here introduce the mapping operator for 2-D signals.Let

$$\begin{aligned} A_1(\omega_1) &\triangleq [a_1(1,\omega_1), a_1(2,\omega_1), ..., a_1(N_f,\omega_1)] \\ A_2(\omega_2) &\triangleq [a_2(1,\omega_2), a_2(2,\omega_2), ..., a_2(N_f,\omega_2)]. \end{aligned} \tag{17}$$

By definition of $\tilde{A}(\omega)$, we have

$$\tilde{A}(\omega) = A_1(\omega_1) \odot A_2(\omega_2). \tag{18}$$

To construct the desired mapping operator, we make the following definitions

$$\begin{aligned} z_1 = z_1(\omega_1) &\triangleq [1, \exp(j2\pi\omega_1), ..., \exp(j2\pi\omega_1 N_f(N_1-1))]^T \\ z_2 = z_2(\omega_2) &\triangleq [1, \exp(j2\pi\omega_2), ..., \exp(j2\pi\omega_2 N_f(N_2-1))]^T, \end{aligned} \tag{19}$$

where $z_1 \in \mathbb{C}^{\widetilde{N_1}}$, $z_2 \in \mathbb{C}^{\widetilde{N_2}}$, $\widetilde{N_1} \triangleq N_f(N_1-1)+1$, $\widetilde{N_2} \triangleq N_f(N_2-1)+1$. Let

$$\begin{aligned} Z_1 = Z_1(\omega_1) &\triangleq [z_1, z_1, ..., z_1] \in \mathbb{C}^{\widetilde{N_1} \times N_f} \\ Z_2 = Z_2(\omega_2) &\triangleq [z_2, z_2, ..., z_2] \in \mathbb{C}^{\widetilde{N_2} \times N_f} \end{aligned} \tag{20}$$

and

$$Z = Z(\omega) \triangleq Z_1(\omega_1) \odot Z_2(\omega_2) = [z, z, ..., z] \in \mathbb{C}^{\widetilde{N_1}\widetilde{N_2} \times N_f}, \tag{21}$$

where $z \triangleq z_1 \otimes z_2$.

Upon examining equations (18) through (21), it becomes apparent that $\tilde{A}(\omega)$ may be regarded as a partial observation of $\tilde{Z}(\omega)$. Consequently, we define the mapping operator $\mathcal{R}$ such that

$$\tilde{A} = \mathcal{R}(\tilde{Z}), \quad \mathcal{R}: \quad \widetilde{N_1}\widetilde{N_2} \times N_f \to N_1 N_2 \times N_f. \tag{22}$$

Let

$$\tilde{X}' \triangleq \sum\nolimits_\omega c_\omega Z(\omega) \odot {p_\omega}^H. \tag{23}$$

It yields from (7), (22) and (23) that $\tilde{X} = \mathcal{R}(\tilde{X}')$. Let

$$\begin{aligned} H &= \mathcal{R}^*(Q) \\ Q &= \mathcal{R}(H). \end{aligned} \tag{24}$$

Substitute (24) into the definition of $\Psi(Q,\omega)$, we obtain

$$\Psi(Q,\omega) = H^H z. \tag{25}$$

(16) thus becomes

$$\|Q\|_{\mathbb{A}}^* = \sup_\omega \|H^H z\|_2, \tag{26}$$

which shows that

$$\|Q\|_{\mathbb{A}}^* \le 1 \quad \Leftrightarrow \quad \|H^H z\|_2 \le 1, \quad \forall\omega. \tag{27}$$

It is important to note that the right-hand side of equation (27) constitutes a multivariate trigonometric polynomial inequality. By invoking the bounded lemma [30] for multivariate trigonometric polynomials and applying an appropriate sum-of-squares relaxation, this inequality can be reformulated into the subsequent semi-definite programming (SDP) problem

$$\begin{aligned} &\delta_k = Tr[\Theta_k P_0], k \in \mathcal{H} \\ &\begin{bmatrix} P_0 & H \\ H^H & I_{N_f} \end{bmatrix} \succcurlyeq 0, \end{aligned} \tag{28}$$

where $\mathcal{H}$ is half space, $\Theta_k = \Theta_{k_1} \otimes \Theta_{k_2}, k = [k_1, k_2]$. Θ_{k_i} is an $\widetilde{N_i} \times \widetilde{N_i}$ Toeplitz matrix with ones on the k_i-th diagonal and 0 elsewhere, $i = 1, 2$. Then (13) can be converted into an SDP as follows

$$\begin{aligned} &\max\nolimits_{Q,P_0,H} < \tilde{X}, Q >_{\mathbb{R}} \quad s.t. \\ &\delta_k = Tr[\Theta_k P_0], \quad k \in \mathcal{H} \\ &\begin{bmatrix} P_0 & H \\ H^H & I_{N_f} \end{bmatrix} \succcurlyeq 0 \\ &H = \mathcal{R}^*(Q). \end{aligned} \tag{29}$$

The semi-definite programming (SDP) formulation of the primal problem (10) is derived from the dual problem of (29). Owing to the constraints of space, we present the result directly. The specified SDP is given as follows

$$\begin{aligned} &\min\nolimits_{W,\mu,\tilde{X}^\clubsuit} \quad \frac{1}{2}[Tr(W) + Tr(Toep(\mu))] \quad s.t. \\ &\begin{bmatrix} Toep(\mu) & \tilde{X}^\clubsuit \\ \tilde{X}^{\clubsuit H} & W \end{bmatrix} \succcurlyeq 0 \\ &\tilde{X} = \mathcal{R}(\tilde{X}^\clubsuit), \end{aligned} \tag{30}$$

where $Toep(\mu)$ is a 2-level multi-level Toeplitz matrix and $\mu \in \mathbb{C}^{\widetilde{N_1} \times \widetilde{N_2}}$.

The angular frequency vector $\omega = [\omega_1, \omega_2]$ can be extracted from $Toep(\mu)$ using the MaPP technique, as proposed in [28]. Subsequently, the elevation and azimuth angles can be estimated by the equations

$$\theta = \arcsin(\sqrt{\omega_1^2 + \omega_2^2} \cdot \frac{c}{f_0 d}) \tag{31}$$

and

$$\phi = \arctan(\frac{\omega_2}{\omega_1}), \tag{32}$$

respectively.

IV. Simulation Results

To evaluate the efficiency of the proposed algorithms, we conducted a series of numerical experiments. Consider a scenario where three underwater acoustic waves impinge upon a 5×5 hydrophone uniform rectangular array (URA). The azimuth and elevation angles are set to $(-60^\circ, -45^\circ, -30^\circ)$ and $(30^\circ, 40^\circ, 45^\circ)$, respectively. The velocity of the underwater sound is assumed to be $v = 1500m/s$. The sound source signals are characterized using the multi-frequency model with a base frequency of $f_0 = 1000Hz$. The spacing between the elements of the array is half of the maximum wavelength, yielding $d = \frac{v}{2f_0}$. The source signals, as defined in (1), are presumed to be independent and are synthesized from a complex normal distribution $\mathcal{CN}(0, I_{N_f})$. The noise is

modeled as white Gaussian noise. The subsequent results are derived from 100 Monte Carlo simulation trials.

In this study, we compare the efficiency of our methodology with that of the conventional atomic norm minimization (ANM)-based narrowband approach, which can be regarded as a particular instantiation of our method with $N_f = 1$. In our algorithm, we set $N_f = 5$. In the absence of noise, the estimation outcomes are depicted in Fig. 2. Fig. 2(a) and Fig. 2(b) delineate the comparative analysis of the angular frequency estimation between the narrowband algorithm ($N_f = 1$) and our proposed method. Fig. 2(c) and Fig. 2(d) illustrate the comparison in the estimation of elevation and azimuth angles. Fig. 2 reveals that, by harnessing additional data from multiple frequencies, our approach yields estimations that cluster tightly around the actual values, whereas the narrowband method produces more dispersed results, thereby demonstrating the superior performance of our proposed methodology.

This observation is further corroborated under noisy conditions. With the signal-to-noise ratio (SNR) set to -10 dB, 0 dB, and 10 dB, the tables reflecting the root mean square error (RMSE) of the elevation and azimuth angles, as well as the angular frequencies relative to the SNR, are presented in TABLE I and TABLE II, respectively. From TABLE I and TABLE II, it is evident that the performance of both methods improves as the SNR increases; however, our method exhibits a more pronounced improvement. To explicate the influence of N_f, we plotted the RMSE curve of the angular frequencies as a function of N_f under noise-free conditions, shown in Fig. 3. It can be discerned from Fig. 3 that performance is enhanced with an increase in N_f.

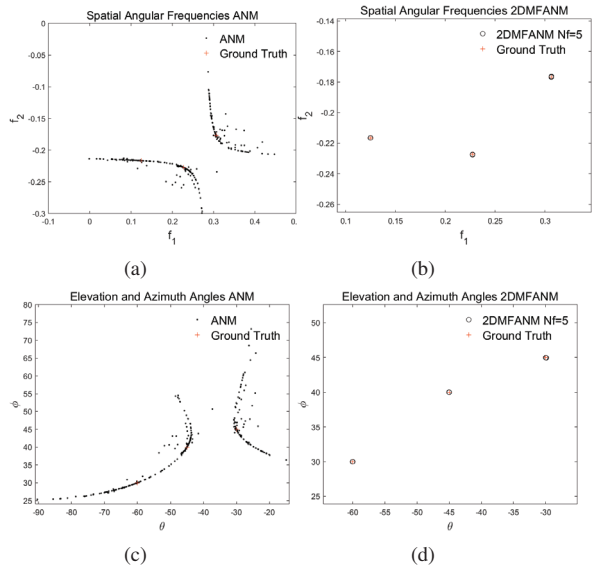

Fig. 2. (a)Estimation of spatial angular frequencies by ANM. (b)Estimation of spatial angular frequencies by 2DMFANM. (c)Estimation of elevation and azimuth angles by ANM. (d)Estimation of elevation and azimuth angles by 2DMFANM

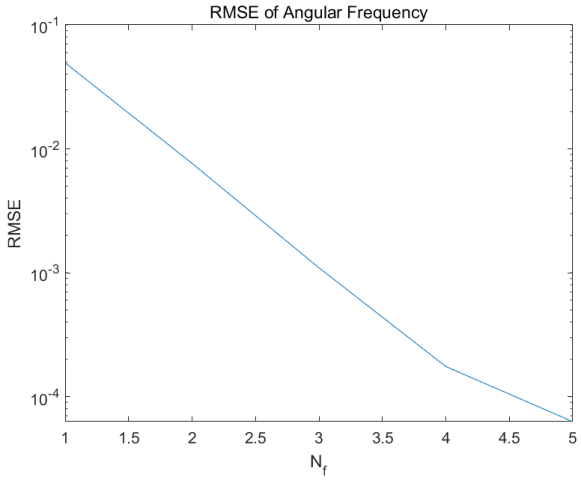

Fig. 3. RMSE of Spatial Angular Frequency

TABLE I
RMSE OF ELEVATION AND AZIMUTH ANGLES

Method	SNR/dB			
	-10	**0**	**10**	**noiseless**
2DMFANM, $N_f = 5$	35.8687	10.5988	0.2287	2.2345×10^{-9}
ANM	45.4704	17.7713	4.0691	0.0420

V. CONCLUSION

In this work, a novel 2DMFANM algorithm is proposed for wideband joint elevation-azimuth angle estimation. The algorithm addresses grid mismatch problems by employing a gridless approach through ANM and leverages the additional information inherent in wideband signals via a multi-frequency model. Compared with traditional narrowband techniques, numerical simulations show that the proposed algorithm significantly enhances estimation precision, maintaining superior performance in both ideal noiseless environments and scenarios where noise in present. It is important to note that a theoretical performance guarantee has not been established within this paper, which remains to be an objective for future research endeavors.

ACKNOWLEDGMENT

This work was supported by the National Natural Science Foundation of China(62371446,62001468,61971412,62201623) and Youth Innovation Promotion Association CAS(2023030).

TABLE II
RMSE OF SPATIAL ANGULAR FREQUENCY

Method	SNR/dB			
	-10	**0**	**10**	**noiseless**
2DMFANM, $N_f = 5$	0.4563	0.2785	0.0998	6.2904×10^{-5}
ANM	0.4327	0.3306	0.1750	0.0494

REFERENCES

[1] H. L. Van, Optimum Array Processing. John Wiley & Sons, 2004.

[2] J. Yang, Y. Yixin, and B. Lei, "An Efficient Compressed Sensing-based DOA Estimation Method in Nested MIMO Sonar," in OCEANS 2017 - ABERDEEN, 2017.

[3] L. Wang, C. Ren, and Z. Zheng, "DOA Estimation for Monostatic Coprime MIMO Radar With Mixed-Resolution Quantization," IEEE Transactions on Vehicular Technology, vol. 72, no. 12, pp. 16737–16741, Dec. 2023, doi: https://doi.org/10.1109/tvt.2023.3293135.

[4] S. Zheng, F. Tong, H. Huang, and Q. Guo, "Exploiting joint sparsity for far-field microphone array sound source localization," Applied Acoustics, vol. 159, pp. 107100–107100, Feb. 2020, doi: https://doi.org/10.1016/j.apacoust.2019.107100.

[5] Chi, Y.; Da Costa, M. Harnessing Sparsity Over the Continuum: Atomic norm minimization for superresolution. IEEE SIGNAL PROCESSING MAGAZINE. 2020 2020 MAR;37(2):39-57.

[6] M. Huan, J. Liang, Y. Wu, Y. Li, and W. Liu, "SASA: Super-Resolution and Ambiguity-Free Sparse Array Geometry Optimization With Aperture Size Constraints for MIMO Radar," IEEE Transactions on Antennas and Propagation, vol. 71, no. 6, pp. 4941–4954, Jun. 2023, doi: https://doi.org/10.1109/tap.2023.3262157.

[7] P. Liu and H. Zhang, "A mathematical theory of computational resolution limit in multi-dimensional spaces *," Inverse Problems, vol. 37, no. 10, p. 104001, Sep. 2021, doi: https://doi.org/10.1088/1361-6420/ac245b.

[8] S. Fortunati, R. Grasso, F. Gini, M. S. Greco, and K. LePage, "Single-snapshot DOA estimation by using Compressed Sensing," EURASIP Journal on Advances in Signal Processing, vol. 2014, no. 1, Jul. 2014, doi: https://doi.org/10.1186/1687-6180-2014-120.

[9] R. Schmidt, A signal subspace approach to multiple emitter location spectral estimation, Ph.D. thesis, Stanford University (1981).

[10] R. Schmidt, "Multiple emitter location and signal parameter estimation," IEEE Transactions on Antennas and Propagation, vol. 34, no. 3, pp. 276–280, Mar. 1986, doi: https://doi.org/10.1109/tap.1986.1143830.

[11] A. Paulraj, R. Roy, and T. Kailath, "A subspace rotation approach to signal parameter estimation," Proceedings of the IEEE, vol. 74, no. 7, pp. 1044–1046, 1986, doi: https://doi.org/10.1109/proc.1986.13583.

[12] E. J. Candes, J. Romberg, and T. Tao, "Robust uncertainty principles: exact signal reconstruction from highly incomplete frequency information," IEEE Transactions on Information Theory, vol. 52, no. 2, pp. 489–509, Feb. 2006, doi: https://doi.org/10.1109/tit.2005.862083.

[13] E. J. Candès, J. K. Romberg, and T. Tao, "Stable signal recovery from incomplete and inaccurate measurements," Communications on Pure and Applied Mathematics, vol. 59, no. 8, pp. 1207–1223, 2006, doi: https://doi.org/10.1002/cpa.20124.

[14] Yang, Z., Li, J., Stoica, P., and Xie, L., "Sparse Methods for Direction-of-Arrival Estimation", arXiv e-prints, 2016. doi:10.48550/arXiv.1609.09596.

[15] Chun-Kit Lai, Shidong Li, Daniel Mondo, Spark-level sparsity and the l1 tail minimization,Applied and Computational Harmonic Analysis, Volume 45, Issue 1, 2018, Pages 206-215, ISSN 1063-5203, https://doi.org/10.1016/j.acha.2017.07.001.

[16] B. Zheng, C. Zeng, S. Li, and G. Liao, "The MMV tail null space property and DOA estimations by tail-l2,1 minimization," Signal Processing, vol. 194, pp. 108450–108450, May 2022, doi: https://doi.org/10.1016/j.sigpro.2021.108450.

[17] Y. Chi, L. L. Scharf, A. Pezeshki, and R. Calderbank, "Sensitivity to basis mismatch in compressed sensing," IEEE Trans. Signal Process., vol. 59, no. 5, pp. 2182–2195, May 2011.

[18] G. Zhang, H. Liu, W. Dai, T. Huang, Y. Liu, and X. Wang, "Passive Joint Emitter Localization with Sensor Self-Calibration," Remote Sensing, vol. 15, no. 3, pp. 671–671, Jan. 2023, doi: https://doi.org/10.3390/rs15030671.

[19] A. Fannjiang and H.-C. Tseng, "Compressive radar with off-grid targets: a perturbation approach," Inverse Problems, vol. 29, no. 5, pp. 054008–054008, Apr. 2013, doi: https://doi.org/10.1088/0266-5611/29/5/054008.

[20] Q. Guo, Z. Xin, T. Zhou, and S. Xu, "Off-Grid Space Alternating Sparse Bayesian Learning," IEEE Transactions on Instrumentation and Measurement, vol. 72, pp. 1–10, Jan. 2023, doi: https://doi.org/10.1109/tim.2023.3243677.

[21] H. Fu, F. Dai, and L. Hong, "Two-Dimensional Off-Grid DOA Estimation with Metasurface Aperture Based on MMV Sparse Bayesian Learning," IEEE Transactions on Instrumentation and Measurement, vol. 72, pp. 1–18, Jan. 2023, doi: https://doi.org/10.1109/tim.2023.3318716.

[22] H. Huang, H. C. So, and A. M. Zoubir, "Off-grid direction-of-arrival estimation using second-order Taylor approximation," Signal Processing, vol. 196, p. 108513, Jul. 2022, doi: https://doi.org/10.1016/j.sigpro.2022.108513.

[23] E. J. Candès and C. Fernandez-Granda, "Towards a mathematical theory of super-resolution," Commun. Pure Appl. Math., vol. 67, no. 6, pp. 906–956, 2014.

[24] G. Tang, B. Bhaskar, P. Shah, and B. Recht, "Compressed sensing off the grid," IEEE Trans. Inf. Theory, vol. 59, no. 11, pp. 7465–7490, 2013.

[25] Firat, U.; Akgul, T. Compressive beamforming for direction-of-arrival estimation of cyclostationary propeller noise. SIGNAL PROCESSING. 2024 2024 JAN;214.

[26] Li, L.; Chen, Y.; Zang, B.; Jiang, L. A High-Precision Two-Dimensional DOA Estimation Algorithm with Parallel Coprime Array. CIRCUITS SYSTEMS AND SIGNAL PROCESSING. 2022 2022 DEC;41(12):6960-6974.

[27] Chi, Y.; Chen, Y. Compressive Two-Dimensional Harmonic Retrieval via Atomic Norm Minimization. IEEE Transactions on Signal Processing. 2015;63(4):1030-1042.

[28] Yang, Z.; Xie, L.; Stoica, P. Vandermonde Decomposition of Multilevel Toeplitz Matrices With Application to Multidimensional Super-Resolution. IEEE Transactions on Information Theory. 2016;62(6):3685-3701.

[29] Wu, Y.; Wakin, M.B.; Gerstoft, P. Gridless DOA Estimation With Multiple Frequencies. IEEE TRANSACTIONS ON SIGNAL PROCESSING. 2023 2023;71:417-432.

[30] Dumitrescu, B. (2007). Positive trigonometric polynomials and signal processing applications. Springer.